



Vegetation, fire and climate change in central-east Isla Grande de Chiloé (43°S) since the Last Glacial Maximum, northwestern Patagonia



O.H. Pesce, P.I. Moreno*

Departamento de Ciencias Ecológicas and Instituto de Ecología y Biodiversidad, Universidad de Chile, Chile

ARTICLE INFO

Article history:

Received 2 December 2013

Received in revised form

20 February 2014

Accepted 26 February 2014

Available online 21 March 2014

Keywords:

Northwestern Patagonia

Southern westerly winds

Last Glacial termination/Holocene

Temperate rainforests

Paleofires

ABSTRACT

We present a detailed record from Lago Lepué to examine vegetation, climate and fire-regime changes since the Last Glacial Maximum (LGM) in central-east Isla Grande de Chiloé (43°S), northwestern Patagonia. Precipitation in this region correlates with the intensity of the southern westerly winds (SWW), allowing reconstruction of past SWW behavior through precipitation-sensitive sensors. Recession from the LGM glacier margins exposed the central-east sector of Isla Grande de Chiloé by 17,800 cal yr BP, followed by the immediate colonization of pioneer cold-resistant herbs/shrubs and rapid establishment of closed-canopy *Nothofagus* forests by 17,000 cal yr BP. Broad-leaved temperate rainforests have persisted since then with compositional changes driven by changes in temperature, hydrologic balance and disturbance regimes. We detect low lake levels and enhanced fire activity between 800–2000, 4000–4300, ~8000–11,000 and 16,100–17,800 cal yr BP, implying southward shifts and/or weaker SWW flow that alternated with cold, humid phases with muted fire activity. Covariation in paleoclimate trends revealed by the Lago Lepué record with tropical and Antarctic records since the LGM, suggests that the SWW have been a highly dynamic component of the climate system capable of linking climate changes from low- and high-southern latitudes during the Last Glacial termination and the current interglacial.

© 2014 Elsevier Ltd. All rights reserved.

1. Introduction

Isla Grande de Chiloé (40–43°S, 71–74°W) (Fig. 1) constitutes the southernmost terrestrial sector of northwestern Patagonia that remained ice-free during the Late Quaternary. Mapping and dating of glacial deposits in its northeastern sector (Denton et al., 1999) have shown that Andean piedmont lobes reached this position during Marine Isotope Stages (MIS) 2 and 4. Although no detailed studies have been conducted in the central and southern sectors of the island, some authors have proposed that glacial margins during the Last Glacial Maximum (LGM = MIS 2) reached more extensive positions further to the west, eventually overriding the coastal range and reaching the Pacific coast south of latitude 42°40'S (Mercer, 1965; Holling and Schilling, 1981). This conjecture led to the idea that ice-free areas in the northwestern portion of the island harbored land biota during the LGM, serving as a source area or corridor for the colonization of exposed ice-free sectors further east and south since the last termination (Heusser, 1990; Villagrán, 2001). The diversity of landscapes and abundant depositional

environments in Isla Grande de Chiloé allow the development of stratigraphic and geomorphic studies to unravel the paleoclimatic and biogeographic evolution through MIS 1–4 along the Pacific coast of mid-latitude South America. Indeed, palynological studies carried out since the 1970s have documented the vegetation and climate history in Isla Grande de Chiloé at multi-millennial scales through the Last Glacial–Interglacial cycle (Godley and Moar, 1973; Heusser and Flint, 1977; Heusser et al., 1981; Villagrán, 1985, 1988a, b; Heusser, 1990; Heusser, 1994; Heusser et al., 1995; Abarzua et al., 2004; Abarzua and Moreno, 2008). Despite the abundance of sites in Isla Grande de Chiloé, none of them offer the stratigraphic continuity, chronologic precision and sampling resolution necessary to examine in detail centennial and millennial-scale changes along a continuum from the LGM to the present. Detailed time series of this type allow examination of the tempo and modes of vegetation, climate and disturbance-regime changes, establishing a bridge between timescales of ecologic and geologic processes. Such data enable the assessment of historical transformations in the context of natural variability under different mean climatic states and transitions.

One of the least understood subjects in Isla Grande de Chiloé is the timing, direction and magnitude of millennial-scale variations

*Corresponding author. Tel.: +56 2 29787391; fax: +56 2 29787315.

E-mail addresses: pimoreno@uchile.cl, pimoreno@vtr.net (P.I. Moreno).

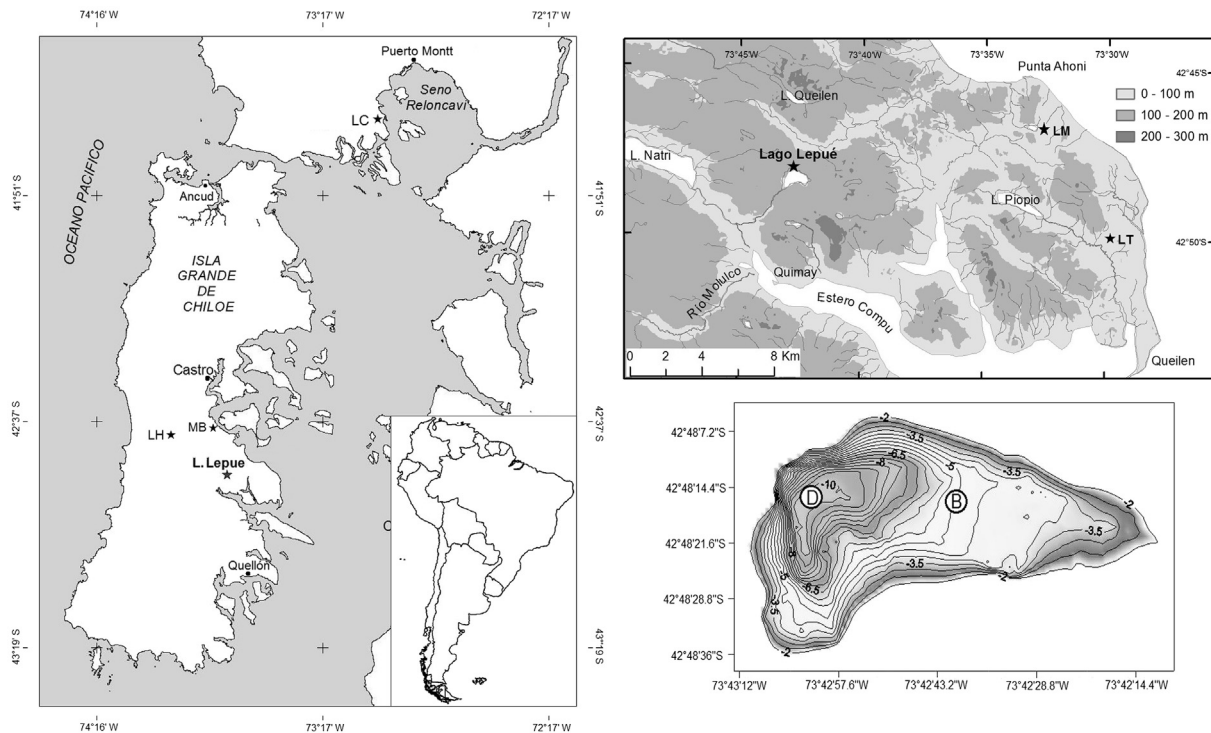


Fig. 1. Map of the study area showing the location of Lago Lepué, its bathymetry, and sites mentioned in the text (LC = Lago Condorito, LH = Lago Huillinco, LM = Lago Melli, LT = Lago Tahui, MB = Mayol Bog). The contours lines in the bathymetry plot are expressed in meters below the lake surface.

in the southern westerly winds (SWW) since the LGM. Recent studies have proposed that the wind-stress imparted by the SWW on the surface of the Southern Ocean is a key factor in the ventilation of CO_2 -rich deep waters, and that the efficiency of this mechanism is modulated by the strength and latitudinal position of the SWW (Toggweiler, 2005; Toggweiler et al., 2006). Empirical support for this hypothesis is afforded by a few records from northwestern and southwestern Patagonia and the Atlantic sector of the Southern Ocean (Heusser et al., 1999; Moreno et al., 1999; Anderson et al., 2009). Limited chronologic precision and temporal resolution of these records, however, impede a closer examination of patterns and processes in particular at millennial and sub-millennial scales. Fire history, a factor closely related to past changes in hydrologic balance and varying degrees of SWW influence (Whitlock et al., 2007; Holz and Veblen, 2012), is also insufficiently understood in northwestern Patagonia as only a handful of sites include analysis of charred microscopic particles (Heusser, 1994) and only one published record from Isla Grande de Chiloé has a contiguous-continuous record of macroscopic charcoal particles (Abarzua and Moreno, 2008). The distinction of particle size in charcoal analysis is an important tool for discriminating local versus regional fires and for deciphering fire-regime changes in the past (Whitlock et al., 2006).

Another subject insufficiently understood is the geography, chronology and ecology of the earliest stages of plant colonization following glacial withdrawal during the last termination. This difficulty stems from the very few records in Isla Grande de Chiloé that span this critical time interval and the lack of sites located in areas adjacent to the putative sources of immigrants. Minimum limiting radiocarbon dates for ice recession from three bogs located in the southern portion of the island (Villagrán, 1985, 1988a, b), an area formerly covered by the Golfo de Corcovado ice lobe, yielded ages of $\sim 15,500$ cal yr BP for the onset of local ice-free conditions, organic sediment accumulation and subsequent spread of arboreal

vegetation, lagging behind chronologies from the mainland by ~ 2200 years. Two recent studies based on lake sediment records from areas formerly covered by the central-east portion of the island (Abarzua et al., 2004; Abarzua and Moreno, 2008) yielded minimum limiting ages for ice recession of $\sim 17,000$ cal yr BP lagging behind the mainland by ~ 700 years (Moreno et al., 1999; Moreno and Leon, 2003). These contrasts could represent heterogeneous responses of Andean ice lobes located at different latitudes and sources driven by climatic contrasts, glaciological differences, residual ice masses left behind during ice recession or, alternatively, stratigraphic heterogeneities and chronologic imprecision in various depositional settings. Resolving these issues will aid in understanding the patterns, magnitude and rapidity of ice recession and plant colonization in this sector of northwestern Patagonia.

The timing, structure and relative magnitude of climate reversals through the Last Glacial termination are controversial subjects that still linger in the discussion after 4 decades of radiocarbon-dated studies in Patagonia. Discussion of the topic has been hampered by the paucity of detailed stratigraphies and chronologies from sensitive sectors over a broad, climatically and biologically diverse region spanning ~ 2000 km along a north-south axis. Recent studies throughout Patagonia suggest a reversal in the deglacial warming trend with a cooling at $\sim 14,500$ cal yr BP (Moreno et al., 2001; Moreno and Leon, 2003; Lamy et al., 2004; Moreno et al., 2012), contemporaneous with glacial readvances/stillstands (Moreno et al., 2009; Sagredo et al., 2011; Stern et al., 2011; Strelin et al., 2011; Garcia et al., 2012) and the onset of the Antarctic Cold Reversal (Stenni et al., 2010). A more heterogeneous picture is evident at the end of the Last Glacial termination, with some records showing either additional cooling and decline in precipitation during the Huelmo-Mascardi Cold Reversal (Hajdas et al., 2003; Moreno and Leon, 2003) or Younger Dryas time (Moreno et al., 1999, 2001), or warming (Lamy et al., 2004) and

glacial recession during Younger Dryas time (Moreno et al., 2009; Sagredo et al., 2011; Stern et al., 2011; Strelin et al., 2011; Garcia et al., 2012). Some records, on the other hand, have been interpreted as showing no indications of climate reversals through the Last Glacial termination (Bennett et al., 2000; Markgraf and Huber, 2011; Markgraf et al., 2013).

Deciphering the anatomy of changes in the SWW is key for assessing the influence of tropical and high-latitude forcing on their position and strength during the Last Glacial termination (Denton et al., 2010) and for testing hypotheses that emphasize their role in the ventilation of deep waters in the Southern Ocean region (Toggweiler et al., 2006; Toggweiler, 2009). In this study we present a fine-resolution pollen and charcoal record from Lago Lepu e to examine millennial and centennial-scale vegetation, climate and fire-regime shifts over the last 17,800 years in central-east Isla Grande de Chilo e. These data allow assessment of the following questions: (1) When did ice-free conditions begin in central-east Isla Grande de Chilo e during the Last Glacial termination? (2) How fast did forest vegetation establish thereafter?; (3) Was the deglacial warming trend a monotonic/unidirectional process?, i.e. were there any climate reversals? if so, what were their timing, structure and magnitude?; (4) How did the SWW vary through the transition from extreme glacial to extreme interglacial conditions?; (5) Is there evidence for high-frequency changes in the SWW during the Holocene?; and (6) How did fire regimes shift through these transitions or climatic states?

1.1. Study area

Isla Grande de Chilo e is the largest island of the Chilotan archipelago, which is located in the southwestern portion of the Chilean Lake District (Fig. 1). The island is separated from the mainland by Canal de Chacao along its northern limit; it faces the Pacific Ocean on the west and the Golfo de Ancud and Golfo de Corcovado along its eastern and southern shores, respectively. The western portion of the island features the Coastal Range, with maximum elevations reaching up to 800 m in its northern half and 500 m in its southern sector.

The climate of northwestern Patagonia is temperate and humid, with increasing precipitation and maritime influence toward the southern and western sectors of the Chilean Lake District. Precipitation at regional scale is delivered exclusively by frontal storms embedded in the SWW belt, thanks to the effective barrier established by the Andes Cordillera to the westward advection of moisture-laden air masses originating from the Atlantic seaboard. Seasonal and year-round positive correlations between zonal wind speeds and local precipitation attest for a close relationship between hemispheric-scale atmospheric circulation and regional climate (Garreaud, 2007; Moy et al., 2008). Hence northwestern Patagonia, and the Chilean Lake District in particular, is a strategic sector to monitor past changes in the SWW through hydroclimate variations based on stratigraphic records. Mean annual temperature measured in Puerto Montt is 10.3  C (14.3–6.5  C: mean monthly temperature in January and July), in Ancud is 11.1  C (15–7.5  C), Castro is 10.5  C (14–6.8  C) and Quell on is 11.3  C (15.1–7.7  C) (Fig. 1). Precipitation in Isla Grande de Chilo e occurs year-round with maximum recorded values during winter and minimum during summer, as a consequence of equatorward- and poleward-shifted SWW through the annual cycle respectively. Mean annual precipitation measured in Puerto Montt is 1765 mm (82–236 mm: mean monthly precipitation in February and June), in Ancud is 2757 mm (110–391 mm), Castro is 1891 mm (74–289 mm) and Quell on is 1960 mm (111–264 mm). The orographic effect of the Coastal Range is evident when comparing the amount of annual rainfall along its western and eastern slopes (>4000

versus ~2000 mm respectively, Direcci on General de Aguas (1987)). At the same latitude on the western slopes of the Andes precipitation is substantially higher, as indicated by the Chait en meteorological station which records mean annual precipitation of 3620 mm (182–447 mm) near sea level. No measurements are available at higher elevations in the Andes, sectors where mean annual precipitation estimates surpass ~5000 mm. Superimposed upon this climatologic mean there is significant variability associated with El Ni o-Southern Oscillation and the Southern Annular Mode, manifested as negative correlations with summer precipitation (Montecinos and Aceituno, 2003; Quintana and Aceituno, 2012).

The dominant vegetation units in northwestern Patagonia are temperate evergreen broad-leaved rainforests from sea level up to the timberline. Latitudinal and altitudinal gradients in temperature and precipitation, coupled with the ruggedness of the terrain, induce segregation of the vegetation into different plant communities which occupy various climatic and geographic zones at regional scale. Descriptions of the floristic composition and physiognomy of these plant communities can be found in Villagr an (1985). In the following section we provide a succinct characterization in terms of their most salient floral and palynological elements in Isla Grande de Chilo e.

1. Valdivian rainforest: This unit is distributed in the lowlands of northern and central Isla Grande de Chilo e up to 250 m a.s.l., with a southern limit of distribution located in Lago Huillinco (Fig. 1). *Eucryphia cordifolia*, *Gevuina avellana* and *Aextoxicon punctatum* are species characteristic of this forest.
2. North Patagonian rainforest: distributed between 200 and 450 m a.s.l. throughout Isla Grande de Chilo e, features dominance of *Nothofagus dombeyi*, *Laureliopsis philippiana*, species of the Myrtaceae and *Weinmannia trichosperma*. Its distribution at higher elevations reflects the ability to tolerate or withstand higher precipitation regimes and lower temperatures than the Valdivian rainforest.
3. Subantarctic Rainforest: dominant above 450 m a.s.l. in the Coastal Range of Isla Grande de Chilo e with the trees *N. dombeyi*, *Nothofagus betuloides*, *Nothofagus nitida* associated with the hygrophilous and cryophilic conifers *Saxegothaea conspicua*, *Podocarpus nubigena*, *Fitzroya cupressoides* and *Pilgerodendron uviferum*, which are often associated with *Drimys winteri* and the herb *Lycopodium magellanicum*.

Our study site, Lago Lepu e, is located in a sector of central-east Isla Grande de Chilo e (42 48'16.01"S, 73 42'49.37" W, 124 m a.s.l.) dominated by secondary growth North Patagonian rainforest trees. Local disturbance by logging and fire is moderate and focused near the northern part of the lake, pasturelands are evident at ~5 km from the site.

2. Materials and methods

We obtained multiple overlapping sediment cores from an anchored raft in Lago Lepu e using a 5-cm diameter Wright piston corer and a 7.5-cm diameter sediment–water interface corer. Sediment descriptions are based on texture and X-radiographs to detect subtle changes and stratigraphic structures. The organic, siliclastic, and carbonate content of the sediments was determined by loss-on-ignition analysis of 1 cc of sediment samples through sequential burns at 550  C for 2 h and 925  C for 4 h. The chronology of the record is constrained by 27 AMS radiocarbon dates on bulk sediment or plant macrofossils.

We processed 1-cc sediment samples for palynological analysis spaced every 2 or 6 cm between levels using standard procedures

(Faegri and Iversen, 1989) that included deflocculating with 10% KOH, sieving (106 μm), 48% HF and acetolysis. We added a known number of exotic *Lycopodium* spores just before acetolysis for calculating pollen concentration and accumulation rate. We counted at least 300 pollen grains of terrestrial origin (trees and shrubs) per level, along with fern spores and pollen of aquatic plants. The abundance of aquatic pollen is expressed as percentages of the total pollen sum (terrestrial + aquatic), the percent abundance of spores was calculated from the sum total pollen + spores. We defined pollen zones to facilitate the description of the pollen record based on visual inspection, aided by a stratigraphically Constrained Incremental Sum of Squares (CONISS) that included all terrestrial pollen taxa with $\geq 2\%$. We analyzed the pollen-slide content of microscopic charcoal (<106 μm) and the abundance of macroscopic charcoal particles on contiguous 1-cm thick 2-cc sediment

samples along the cores. The latter were deflocculated in 10% KOH, rinsed carefully and sieved into fractions >212 and >106 μm . All charcoal data are expressed as accumulation rates (particles/ $\text{cm}^2\cdot\text{year}$).

3. Results

We obtained sediment cores from the deepest (10 m water depth, core 0403SC + 0403AT1 + 0201D) and intermediate (5.5 m water depth, core 0201B) sectors of Lago Lepu  (Fig. 2). We conducted pollen and charcoal analyses on a spliced 1250-cm long record that combines overlapping sediment–water interface and Wright cores obtained from the deepest sector of the lake. The stratigraphy shows predominance of organic lake mud (gyttja) devoid of carbonates (<5%) that grades downward into organic

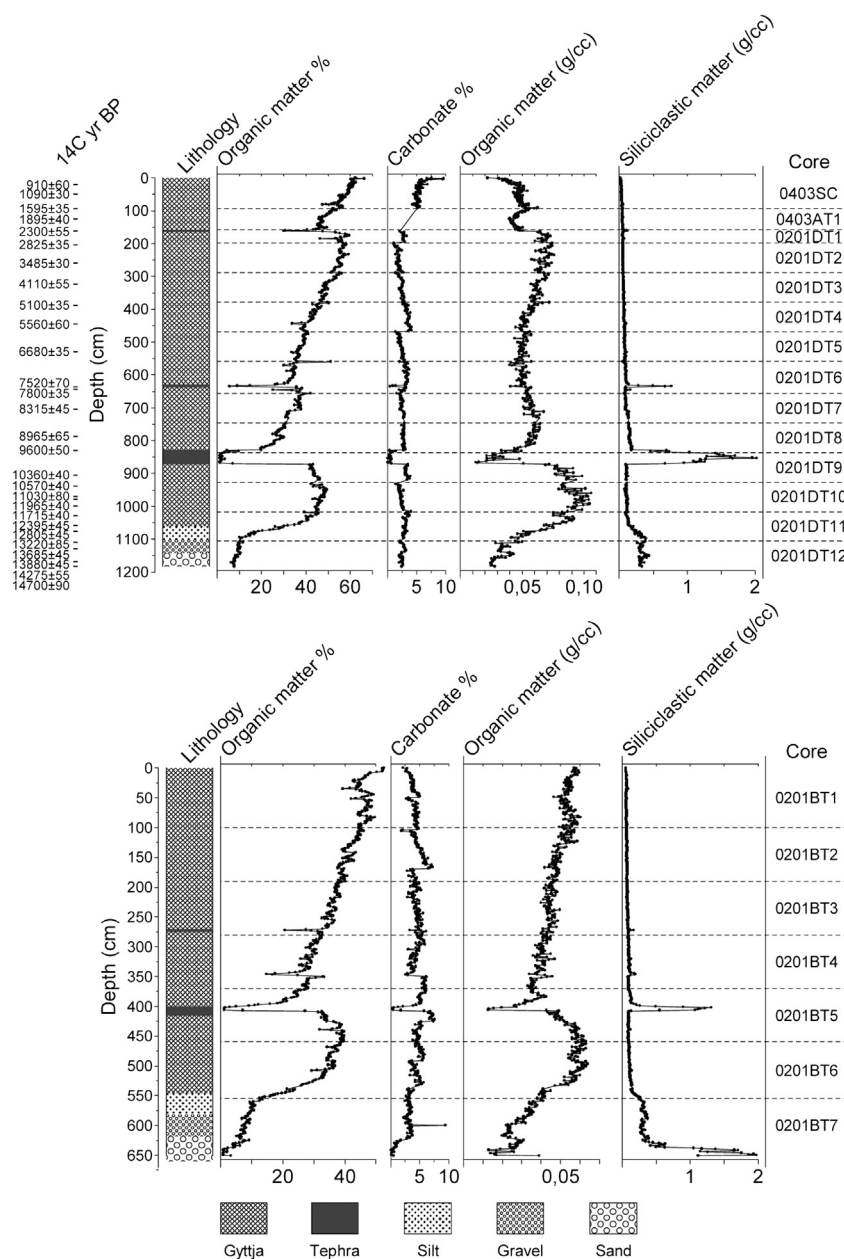


Fig. 2. Stratigraphic column, radiocarbon dates, selected loss-on-ignition parameters, depth span and identity of sediment cores collected from the deep and intermediate sectors of Lago Lepu , core series 0201D and 0201B respectively. The radiocarbon date labels are slightly offset relative to their position in the core to facilitate visualization.

silts, sands and basal gravel. We found three tephra in core 0201D at 156, 626 and 826 cm, having 3, 7 and 44 cm in thickness, respectively. Our chronology (see below) indicates ages of 2250, 8300 and 11,000 cal yr BP for these volcanic ashes, respectively. The deepest tephra is an andesite probably originating from Volcán Michinmahuida. Its considerable thickness and bedding suggests intense reworking during a particularly low lake level stand, aspect we will discuss in a subsequent section of this paper. A nearly identical stratigraphy is evident in core 0201B, which has a length of 650 cm. The radiocarbon dates suggest undisturbed, continuous deposition and high accumulation rate of lake mud over the last 17,800 years (Table 1). We developed a Bayesian age model using Bacon (Blaauw and Christen, 2011) (Fig. 3) to assign interpolated ages to all levels analyzed, after subtracting the thickness of all tephras considering their instantaneous deposition. This model indicates a median deposition time of 15 yr/cm throughout the record. The excellent match between the dated core (spliced 0201D) and the undated core (0201B) allowed us to transfer the interpolated ages produced by the age model based on tephras-stratigraphy and conspicuous variations in the organic density curves (Fig. 4). The striking resemblance between records is evident even for subtle centennial-scale variations, in particular during the interval between 2300 and 7800 cal yr BP, suggesting that sedimentation at intermediate and deep sectors of Lago Lepué was identical ~80% of the time over the last 17,800 years. Divergence between cores is evident between 1400–2300 and 7800–11,000 cal yr BP (Fig. 4), which we interpret as downslope migrations of the sediment limit associated with regressive lake-level phases, causing depositional/erosional heterogeneities between the cored sectors (Shuman, 2003). We will return to this aspect in the context of the pollen and charcoal records in a subsequent section of this paper.

3.1. Fossil pollen

The pollen record from Lago Lepué consists of 417 levels that span the last 17,800 years, with a mean time step of 43 years

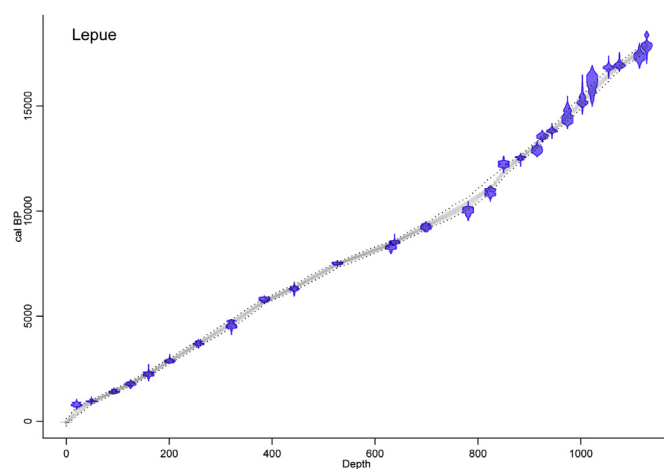


Fig. 3. Age model from core 0403SC+0403AT1+0201D constructed using Bacon. The x axis corresponds to the tephra-free depth of the spliced record. The probability distribution of each calibrated radiocarbon date is shown in blue, the gray pattern represents the 95% confidence interval of the Bayesian age model. (For interpretation of the references to colour in this figure legend, the reader is referred to the web version of this article.)

between samples. In the following section we describe the pollen record, which we divided in 13 zones based on the major changes in pollen stratigraphy and a stratigraphically constrained CONISS analysis (Figs. 5 and 6). The nomenclature of these zones reflects the three most abundant terrestrial pollen taxa in decreasing order from the most abundant taxon.

Zone LL1 (1119–1182 cm, 16,700–17,800 cal yr BP) features the assemblage *Nothofagus*-*Poaceae*-*Ericaceae*. Arboreal pollen is the lowest (20%) at the base owing to peak of abundance of *Poaceae*, *Ericaceae*, *Asteraceae* subfamily *Asteroidae* and *Gunnera*, accompanied by the pteridophytes *Blechnum*, *Pteris* and *L. magellanicum*. This situation reverses toward the end of this zone with the appearance of *Drimys* and *Escallonia* and peak abundance of *Nothofagus* and *Misodendrum* along with minimum abundance of

Table 1

Information on the radiocarbon dates from Lago Lepué. All dates were obtained using the AMS dating technique, radiocarbon age calibrations were performed using CALIB 6.01. The modified depths were obtained by subtracting the tephra thicknesses from the original depth.

Laboratory code	Core	Original depth (cm)	Modified depth (cm)	^{14}C yr BP $\pm 1\sigma$	Median probability (cal yr BP)	2σ intercepts (cal yr BP)
CAMS-124560	0403SC	20	20	910 \pm 60	781	681–908
CAMS-124561	0403SC	49	49	1090 \pm 30	948	909–1052
CAMS-125907	0403AT1	93	93	1565 \pm 35	1392	1313–1517
CAMS-125908	0201DT1	125	125	1895 \pm 40	1776	1631–1880
ETH-26144	0201DT1	162	158	2300 \pm 55	2235	2122–2351
CAMS-125909	0201DT2	203	199	2825 \pm 35	2864	2775–2958
CAMS-125910	0201DT2	259	255	3485 \pm 30	3684	3582–3827
ETH-26145	0201DT3	323	319	4110 \pm 55	4553	4415–4815
CAMS-125911	0201DT4	387	383	5100 \pm 35	5810	5663–5904
ETH-26146	0201DT4	445	441	5560 \pm 60	6305	6184–6436
CAMS-125912	0201DT5	529	525	6680 \pm 35	7513	7438–7572
ETH-25450	0201DT6	636	632	7520 \pm 70	8279	8065–8410
CAMS-125913	0201DT6	643	634	7800 \pm 35	8519	8429–8592
CAMS-125914	0201DT7	704	695	8315 \pm 45	9244	9035–9420
ETH-25451	0201DT8	786	777	8965 \pm 65	10,022	9770–10,221
CAMS-125915	0201DT9	904	854	10,360 \pm 40	12,222	12,062–12,394
CAMS-146702	0201DT10	937	887	10,570 \pm 40	12,538	12,421–12,618
ETH-26147	0201DT10	969	919	11,030 \pm 80	12,913	12,689–13,107
CAMS-125916	0201DT10	979	929	11,715 \pm 40	13,562	13,414–13,722
CAMS-146703	0201DT10	998	948	11,965 \pm 40	13,823	13,710–13,962
CAMS-146704	0201DT11	1028	978	12,395 \pm 45	14,440	14,106–14,934
CAMS-146705	0201DT11	1057	1007	12,805 \pm 45	15,218	14,911–15,651
ETH-25453	0201DT11	1076	1026	13,220 \pm 85	16,136	15,373–16,693
CAMS-146706	0201DT12	1108	1058	13,685 \pm 45	16,826	16,660–16,996
CAMS-125917	0201DT12	1129	1079	13,880 \pm 45	16,950	16,781–17,148
CAMS-146707	0201DT12	1168	1118	14,275 \pm 55	17,358	17,023–17,667
ETH-25455	0201DT13	1182	1132	14,700 \pm 90	17,884	17,558–18,473

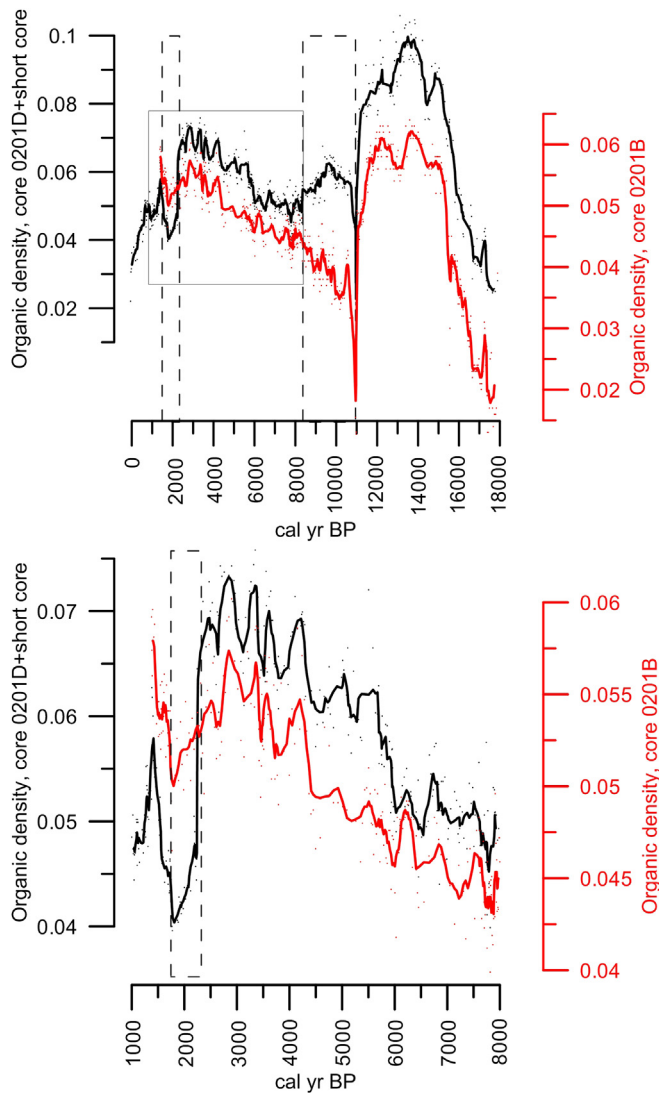


Fig. 4. Organic density variations from cores 0201D and 0201B expressed in a common timescale. The individual values are shown as small dots, the solid lines represent weighted 7-point weighted running means applied to each record. The dashed rectangles identify intervals of major divergence between cores, the solid line rectangle corresponds to the zoomed interval shown in the lower panel.

Poaceae, Ericaceae and Asteraceae subfamily Asteroidae. The microalgae *Botryococcus* and *Pediastrum* attain their highest percentages of the entire record at the beginning of this zone, subsequently decreasing to 15%; *Isoetes* increases its dominance reaching 15%.

Zone LL2 (1074–1119 cm, 15,800–16,700 cal yr BP) is dominated by the assemblage *Nothofagus*-Poaceae-*Fitzroya/Pilgerodendron*. *Nothofagus* declines to 40% at 16,500 cal yr BP and then increases until ~60% at the end of the zone, *Drimys* increased slightly while *Fitzroya/Pilgerodendron* rises steadily to 23%. Ericaceae and Poaceae increase between 16,500 and 16,800 cal yr BP, and then diminish to their minimum abundance. *Blechnum*, *Pteris* and *L. magellanicum* reach their maximum abundance of the entire record during this zone at 16,500 cal yr BP. *Botryococcus* and *Pediastrum* increase their percentage at 16,500 cal yr BP, after that, decreased to 7% at the end of this zone. *Isoetes* decreases steadily throughout this zone.

Zone LL3 (1026–1074 cm, 14,600–15,800 cal yr BP) is dominated by the *Nothofagus*-Myrtaceae-*Fitzroya/Pilgerodendron* assemblage. Myrtaceae increases rapidly from 16,100 cal yr BP onward

accompanied by *Griselinia*, *Lomatia/Gevuina*, *Embothrium coccineum* and *Fuchsia*, while Poaceae, *Fitzroya/Pilgerodendron*, Ericaceae, *Blechnum*, *L. magellanicum* and *Isoetes* plummet to virtually disappear. *Raukaua laetevirens* and *Drimys* reach their maximum abundance of the entire record during this zone.

Zone LL4 (949–1026 cm, 12,900–14,600 cal yr BP) is characterized by the assemblage *Nothofagus*-Myrtaceae-*P. nubigena*. *P. nubigena* rises steadily to its maximum (~35%) at 12,600 cal yr BP, contemporaneous with notable declines in *Fitzroya/Pilgerodendron*, *Nothofagus* Myrtaceae, *R. laetevirens* and *Drimys*. *Hydrangea* exhibits a gradual and steady rise, along with a slight and variable increase in *Misodendrum*.

Zone LL5 (890–949 cm, 11,600–12,900 cal yr BP) is dominated by the assemblage *P. nubigena*-*Nothofagus*-Myrtaceae. *P. nubigena* starts this zone with peak abundance and declines to about half its initial value by 11,700 cal yr BP, while Myrtaceae, *Hydrangea*, and *Tepualia stipularis* increase altogether. All other terrestrial taxa exhibit abundances below 4%.

Zone LL6 (669–890 cm, 8008–11,600 cal yr BP) features the assemblage *Hydrangea*-Myrtaceae-*W. trichosperma*. *Hydrangea* continues its increase until a maximum of 52% at 10,500 cal yr BP, and declines gradually thereafter. Myrtaceae shows an increase from ~15% to ~30%, in contrast *Nothofagus* decreases to its all-time minimum (~15%), while *P. nubigena*, *Fitzroya/Pilgerodendron*, *Drimys* and *T. stipularis* virtually disappear. *W. trichosperma* increases abruptly reaching a plateau with fluctuations between 20 and 40%, and then decreases to 12%. During this zone *Eucryphia/Caldcluvia* presents brief, intermittent, low-magnitude increments (<10%), concomitant with a prominent increase in *Isoetes* that led to its highest abundance in the entire record. At the same time, the heliophytic fern *Lophosoria quadripinnata* experienced a noteworthy and variable increase up to 3%.

Zone LL7 (475–669 cm, 6700–8800 cal yr BP) features dominance of the assemblage *Nothofagus*-Myrtaceae-*Eucryphia/Caldcluvia*. *Eucryphia/Caldcluvia* increases rapidly and reaches a plateau (~15%), along with gradual and steady increases in *Nothofagus* and *Misodendrum*, reappearance of *P. nubigena*, a rise in *W. trichosperma* and high abundance of *L. quadripinnata*. *Hydrangea*, Myrtaceae, *Isoetes* and *Botryococcus* show major declines.

Zone LL8 (320–475 cm, 4500–6700 cal yr BP) is characterized by the assemblage *Nothofagus*-*Eucryphia/Caldcluvia*-Myrtaceae. *Nothofagus* reaches its maximum abundance in a plateau (~40%), accompanied by increases in *P. nubigena* and *D. winteri*. *Lepidoceras kingii* exhibits an abrupt increase at 6000 cal yr BP, contemporaneous with an increasing trend in *S. conspicua* and a discrete rise in *T. stipularis*. *Eucryphia/Caldcluvia* and Myrtaceae present a clear downward trend, similar to *L. quadripinnata* and *Isoetes*.

Zone LL9 (270–320 cm, 3700–4500 cal yr BP) is defined by the assemblage *Nothofagus*-*Eucryphia/Caldcluvia*-*W. trichosperma* and features a significant decrease in *Nothofagus* reaching 17% at 3900 cal yr BP, while *Eucryphia/Caldcluvia* and *W. trichosperma* increase. Myrtaceae presents average values of 7% and *L. kingii* experiences an abrupt decrease. *S. conspicua* and *P. nubigena* continue their steady increases.

Zone LL10 (180–270 cm, 2500–3700 cal yr BP) is dominated by the assemblage *Nothofagus*-Myrtaceae-*W. trichosperma*. *S. conspicua* and *Drimys* show sustained increases and, to a lesser degree, *P. nubigena*. In contrast, *Eucryphia/Caldcluvia*, *L. kingii*, *L. quadripinnata* and *Isoetes* decline. Myrtaceae begins this zone with 20% and decreases steadily to 10%.

Zone LL11 (114–180 cm, 1700–2500 cal yr BP) features dominance of the assemblage *Nothofagus*-*W. trichosperma*-Myrtaceae. *Nothofagus* shows a reversal that culminates at 2000 cal yr BP, while *W. trichosperma* increased steadily to a maximum of 33%, accompanied by increases in Myrtaceae, *T. stipularis*, *Drimys*, *L. kingii* and

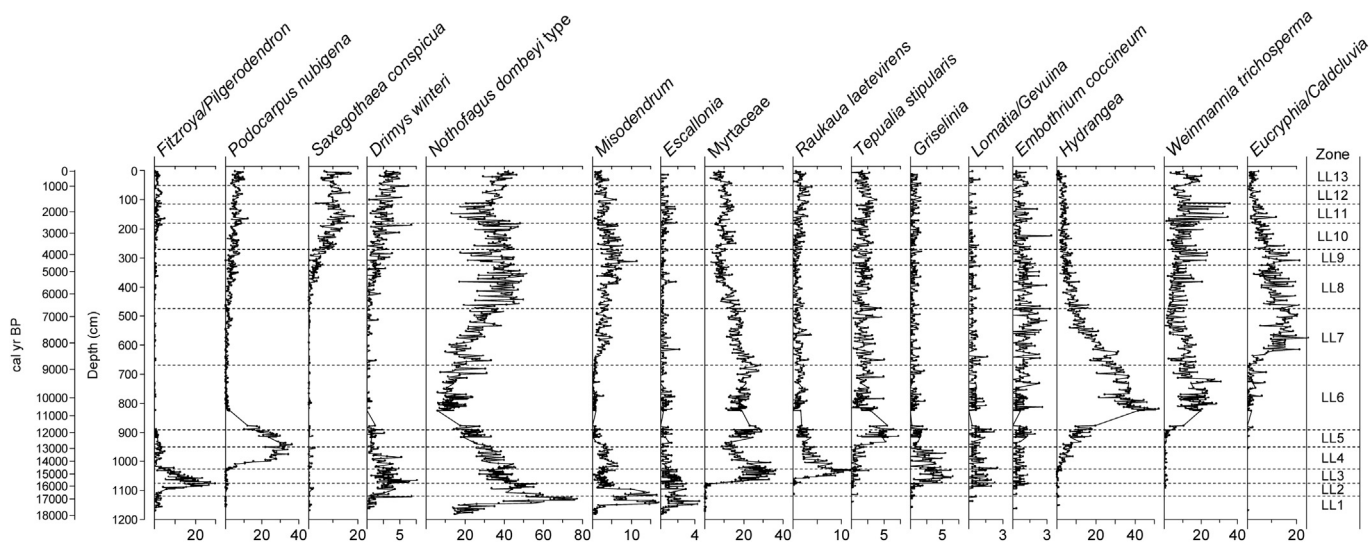


Fig. 5. Pollen percentage diagram of arboreal taxa from Lago Lepué. The dashed horizontal lines define the boundaries of pollen assemblage zones identified with a label on the right side of the diagram. The primary y axis expresses the original depth of the record (including tephra), the secondary y scale expresses the age model.

Isoetes. *S. conspicua* achieves its maximum value (18%) in the record at 2100 cal yr BP, declining afterwards.

Zone LL12 (50–114 cm; 960–1700 cal yr BP) shows a *Nothofagus*–*Myrtaceae*–*W. trichosperma* assemblage, in which *Nothofagus*, *S. conspicua*, *P. nubigena* and *Fitzroya/Pilgerodendron* exhibit rising trends and *W. trichosperma* decreases sharply. *Isoetes* attains a maximum at the beginning of this zone and remains abundant with a slight decline towards the end of this zone.

Zone LL13 (0–50 cm, present–960 cal yr BP) characterized by the *Nothofagus*–*W. trichosperma*–*S. conspicua* assemblage, in which *Nothofagus*, *Drimys*, *Myrtaceae*, *W. trichosperma* and *S. conspicua* increase toward the present.

3.2. Fossil charcoal

The microscopic and macroscopic charcoal accumulation rates (CHAR) (Fig. 7) reveal persistently low or null values throughout the record except for the following increases:

- Discrete peaks of macroscopic CHAR at 16,200 and 17,300 cal yr BP coeval with larger-magnitude increases in microscopic CHAR, followed by conspicuous peaks between 12,500 and 12,900 cal yr BP again with larger magnitude increases in microscopic charcoal.
- Persistently high CHAR between 8900 and 11,000 cal yr BP in both size classes.
- Charcoal peaks at 4000, 4200 and 7700 cal yr BP in both size classes.
- High CHAR between 800 and 2900 cal yr BP. Macroscopic CHAR increases steadily to its maximum abundance at 800 cal yr BP, while the microscopic CHAR shows a peak at 2200 cal yr BP, followed by a sequence of low magnitude peaks, ending with a large-magnitude peak at 1000 cal yr BP.

4. Discussion

The pollen record from Lago Lepué indicates dominance of non-arboreal pollen (chiefly Poaceae, Ericaceae and *Gunnera*) between 17,400 and 17,800 cal yr BP, along with the pteridophyte *L. magellanicum* and the lowest content of organic matter (Figs. 5 and 6). High representation of herbs, shrubs, and the microalgae

Botryococcus and *Pediastrum* at the beginning of the Lago Lepué record reflect the earliest stages of plant colonization in the cold, barren, low-productivity, recently deglaciated landscapes of this sector of Isla Grande de Chiloé, which we interpret as a wind-swept, treeless environment similar to the landscapes found today in the high Andes of northwestern Patagonia where low temperatures and prolonged snow cover limit the occurrence of arboreal vegetation (Heusser et al., 1999). Previous palynological studies from the Chilean Lake District and Isla Grande de Chiloé (Heusser et al., 1999; Moreno et al., 1999) have proposed a 6–7 °C cooling during the coldest intervals of the LGM. This was based on the inference of ~900–1000 m lowering of treeline during the LGM, and an adiabatic lapse rate of 0.65 °C/100 m. The oldest assemblages of the Lago Lepué record are consistent with these interpretations and inferences. We observe an abrupt increase in *Nothofagus* at 17,400 cal yr BP from its lowest (~20%) to its highest (~90%) abundance within ~400 years, accompanied by its hemiparasitic mistletoe *Misodendrum* and the shade-intolerant cold-resistant tree *Drimys* in the context of a pollen assemblage dominated by pioneer cold-resistant herbs and shrubs. High abundance of the macrophyte *Isoetes* between 16,100 and 17,400 cal yr BP suggests that littoral vegetation grew close to the deepest sector of the lake, implying low lake levels at that time. Our data indicate rapid spread and establishment of closed-canopy forests by 17,000 cal yr BP with species found in modern Subantarctic/North Patagonian rainforest communities, suggesting an extraordinarily rapid response of the vegetation to abrupt warming at the beginning of the Last Glacial termination. Evergreen temperate rainforest dominance has persisted in central-east Isla Grande de Chiloé since then, with variations in their structure and composition we interpret as changes in climate and disturbance regimes.

The cold-resistant hygrophilous conifer *Fitzroya/Pilgerodendron* rose at 16,100 cal yr BP along with the tree *Lomatia/Gevuina*, understory ferns (*Blechnum*) and shrubs commonly found in forest edges (*Escallonia*, *Fuchsia*, *Griselinia*, *Aristotelia chilensis*, *E. coccineum*). Shade-tolerant, relatively thermophilic trees (*Myrtaceae*, *R. laetevirens*) and vines (*Hydrangea*) appear in the record at 16,300 cal yr BP and increase abruptly at 15,800 cal yr BP replacing *Nothofagus*, *Drimys*, *Fitzroya/Pilgerodendron* and *Escallonia*, concomitant with marked declines in *Isoetes* and *Blechnum* and a rapid increase in the organic content of the sediments. We interpret

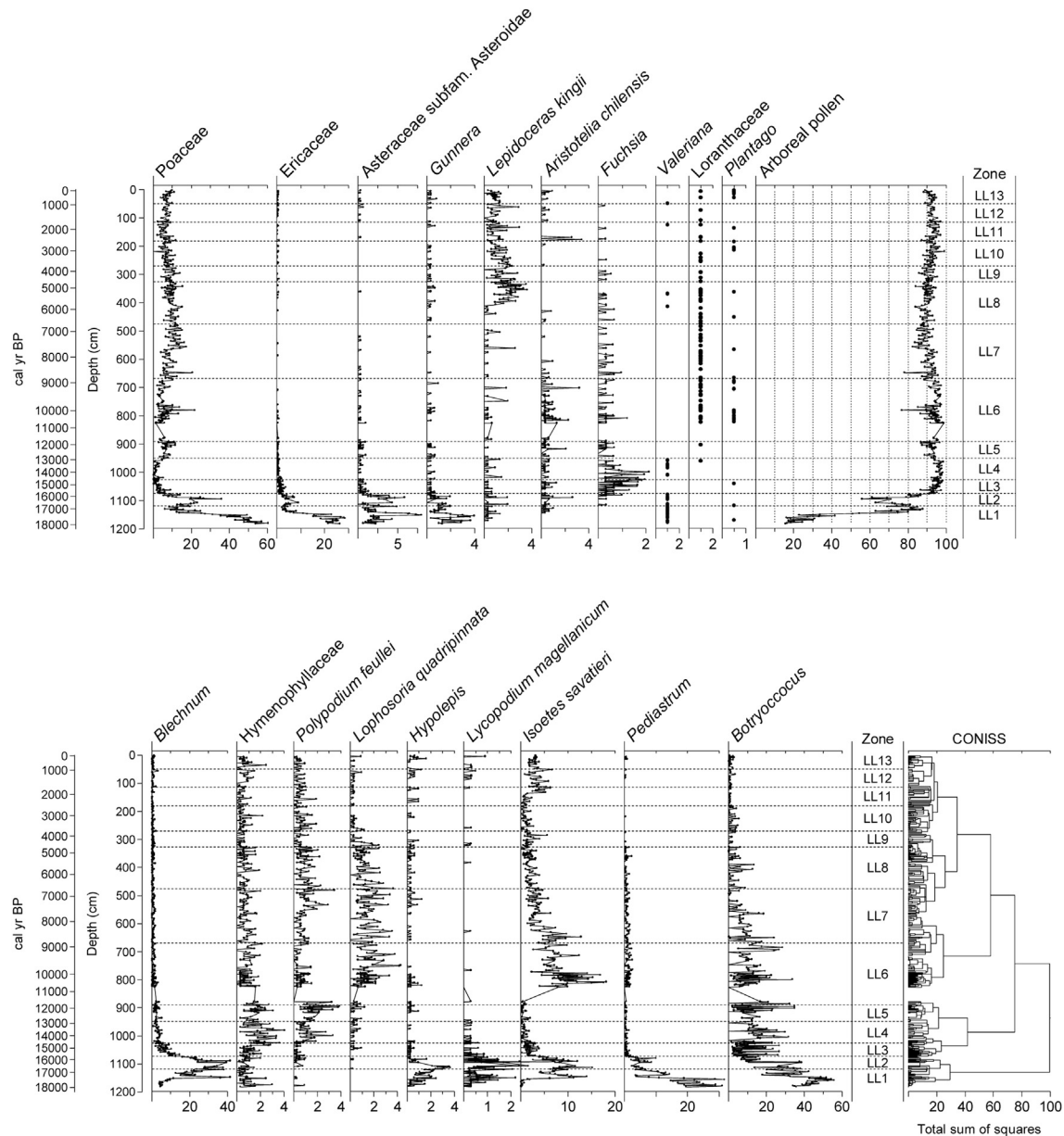


Fig. 6. Upper panel: percentage diagram of non-arboreal taxa and arboreal pollen sum. Lower panel: percent diagram of pteridophytes and microalgae from Lago Lepu , along with results of the CONISS ordination. The dashed horizontal lines define the boundaries of pollen assemblage zones identified with a label on the right side of the diagram. The primary y axis expresses the original depth of the record (including tephras), the secondary y scale expresses the age model.

these changes as shifts in the structure and composition of the forest understory, increased productivity in the lake ecosystem and a rise in lake level that drove littoral macrophyte away from the lake center. This floristic turnover suggests rapid establishment of closed-canopy North Patagonian rainforests driven by warmer conditions between 14,600 and 16,100 cal yr BP. A rapid and large-magnitude increase of the cold-resistant hygrophilous conifer *P. nubigena* occurred between 12,700 and 14,600 cal yr BP, along with the vine *Hydrangea* at the expense of all other trees including the thermophilous Myrtaceae. The modern abundance of *P. nubigena* is highest in North Patagonian rainforest communities located above 450 m a.s.l. in the mountain ranges of Isla Grande de Chilo  and northwestern Patagonia and below the frost-resistant Subantarctic deciduous forests that establish the Andean treeline at regional scale (~1100 m a.s.l.). Thus, we interpret the rise in *P. nubigena* as a reversal toward cooler, wetter climate at times when the lowlands

of Isla Grande de Chilo  were dominated by closed-canopy evergreen temperate rainforests composed exclusively by cryophilic North Patagonian trees and abundant epiphytic ferns (Hymenophyllaceae, *Polypodium feullei*). This interval features peak organic density in the deep and intermediate sectors of Lago Lepu , suggesting a common depositional regime below the sediment limit during high lake-level stands. *P. nubigena* then declined steadily between 11,500 and 12,700 cal yr BP to approximately half its peak abundance as Myrtaceae, *T. stipularis*, *W. trichosperma*, *Hydrangea* and, to a lesser extent, Poaceae increased. The shade-intolerant species *T. stipularis* is a hygrophilous tree commonly found in evergreen North Patagonian and Subantarctic rainforests in upland and waterlogged environments, also present in river and lake edges along with other species of the Myrtaceae family. We interpret the rise in *T. stipularis* and Myrtaceae between 11,500 and 12,700 cal yr BP as indicative of a slight lowering in lake level that

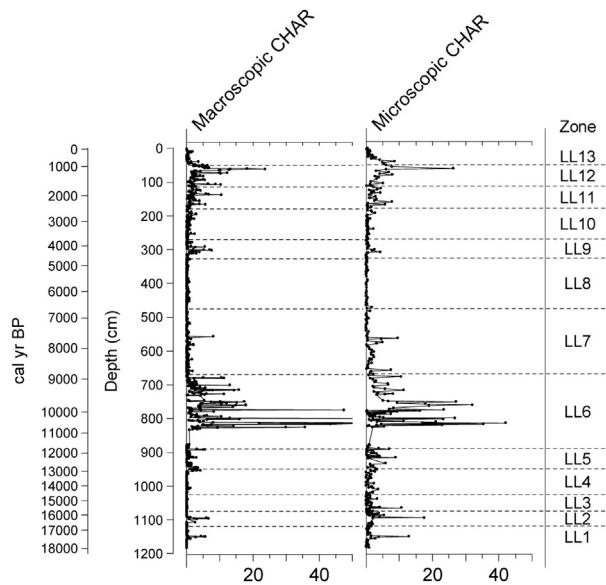


Fig. 7. Accumulation-rate diagrams of microscopic and macroscopic charcoal particles from Lago Lepu . The dashed horizontal lines define the boundaries of pollen assemblage zones identified with a label on the right side of the diagram. The primary y axis expresses the original depth of the record (including tephras), the secondary y scale expresses the age model.

drove the centripetal expansion of swamp environments located in the periphery of Lago Lepu  toward deeper sectors of the lake. In sum, we interpret a reversal toward cooler and wetter conditions between 11,500 and 14,600 cal yr BP, the first part of which featured the largest magnitude decline in temperature and increase in precipitation between 12,700 and 14,600 cal yr BP, followed by cold seasonally dry climate or high frequency of droughts between 11,500 and 12,700 cal yr BP. This interval features declines in organic density in the deep and intermediate sectors of Lago Lepu , decline that is most marked in the sediment core collected from the deep zone.

Major increases in *Hydrangea* and *W. trichosperma* started at 11,600 and 11,100 cal yr BP, respectively, coeval with sustained declines in the cold-resistant *Nothofagus* and *P. nubigena*, signaling a warm phase at the beginning of the Holocene. These changes were contemporaneous with the appearance and modest increase in the thermophilous, summer-drought resistant trees *Eucryphia/Caldcluvia* (characteristic of the lowland Valdivian rainforest) at 11,400 cal yr BP, increments in *L. quadripinnata* (a shade-intolerant fern commonly found in forest edges), a major rise in the littoral macrophyte *Isoetes* that led to peak abundance at 10,600 cal yr BP coeval with substantial declines in organic density at intermediate and deep sectors in the lake and occurred right after the deposition of an andesitic tephra erupted from Volc n Michinmahuida. We note a conspicuous divergence in the organic density data between the intermediate and deep cores between ~8000 and 11,000 cal yr BP, which we attribute to lowering of the sediment limit in response to a regressive lake phase. *Eucryphia/Caldcluvia* increased abruptly at 8600 cal yr BP and reached its maximum (25%) at 7800 cal yr BP. We interpret the record between 7800 and 11,500 cal yr BP as a shift from a North Patagonian-dominated rainforest to woodland dominated by species commonly found in Valdivian rainforests, during a prominent warm/dry phase. These changes occurred immediately after the deposition of the deepest tephra raising the possibility that climate-driven changes in the upland vegetation acted in a synergistic manner with volcanic and fire disturbance (see Section 4.1).

North Patagonian trees (*Nothofagus*, *Drimys* and *P. nubigena*) started a persistent increase at ~7800 cal yr BP, followed by a sustained long-term increase in the podocarp *S. conspicua* and the parasitic epiphyte *L. kingii* at 6200 cal yr BP, while relatively thermophilic trees and vines (*Hydrangea*, Myrtaceae, *Eucryphia/Caldcluvia*) declined, suggesting a shift from a woodland dominated by Valdivian rainforest taxa toward a mixed forest dominated by North Patagonian trees. A contemporaneous increase in the organic density data is evident in the intermediate and deep cores from Lago Lepu , overprinted by prominent centennial-scale oscillations. Our data suggest a multi-millennial cooling trend and increase in precipitation between 2500 and 7800 cal yr BP accompanied by enhanced productivity in the lake. *Nothofagus* achieved a high-abundance plateau between 0 and 6200 cal yr BP, punctuated by reversals between 1700–2500 and 4000–4300 cal yr BP during which *S. conspicua* declined contemporaneous with increases in *W. trichosperma*, *Eucryphia/Caldcluvia* and *Isoetes* defining centennial-scale oscillations we interpret as warm/dry anomalies.

The most recent 2000 years feature preeminence of North Patagonian rainforest trees with vegetation changes consistent with intense disturbance (decline in shade tolerant trees [*S. conspicua*], increase in opportunistic shade-intolerant trees [*W. trichosperma*] and *Isoetes* between 800 and 2000 cal yr BP. We observe a contemporary divergence in the organic density of the sediments in the intermediate and deep sectors of the lake, suggesting a lowering in lake sediment limit and a regressive lake phase.

4.1. Fire history and hydrologic balance

CHAR was very low or absent between 11,000 and 17,800 cal yr BP when cool-wet Subantarctic-North Patagonian rainforests dominated the record. Within this interval we observe intermittent increases at 12,900, 16,200 and 17,300 cal yr BP, indicative of centennial-scale shifts in fire regime at millennial timescales. We attribute these shifts to negative precipitation anomalies, most likely during summer, which allowed desiccation of coarse woody fuels when Subantarctic/North Patagonian rainforests dominated the landscape under cool-temperate and wet conditions. A sustained rise in CHAR between 8900 and 11,000 cal yr BP defines a multi-millennial phase in fire activity which coincided with the spread of shade-intolerant trees and herbs (*W. trichosperma*, Poaceae) and disappearance of hygrophilous cold-resistant conifers (*P. nubigena*, *Fitzroya/Pilgerodendron*) during an extreme multi-millennial warm-dry phase. Fire-related discontinuities in the forest canopy promoted the proliferation of the vine *Hydrangea* in the high-luminosity environments in the woodland edges. Another multi-millennial phase in CHAR is evident between 2900 and 8900 cal yr BP and features little or null fire activity punctuated by discrete low-magnitude charcoal peaks at 4000, 4200, 6200, 7700 cal yr BP. This was followed by sustained multi-millennial increase in CHAR over the last 2900 years with prominent peaks at 800 and 2400 cal yr BP, which we interpreted as a trend toward drier summers.

We observe covariation between CHAR and the littoral macrophyte *Isoetes* during the intervals 800–2400, 3900–4100, 8500–11,500 and 16,100–17,300 cal yr BP, suggesting that enhanced fire activity was contemporaneous with centennial and millennial-scale lake-regressive phases in Lago Lepu  (Fig. 8). The Holocene events were contemporaneous with increases in *W. trichosperma* and declines in *Nothofagus*, which we interpret as forest disturbance by paleofires, and conspicuous divergences between the organic density data from the deep and intermediate sectors of Lago Lepu  between 800–2000 and ~8000–11,000 cal yr BP driven by lowering in sediment-limit depth driven by lake-level

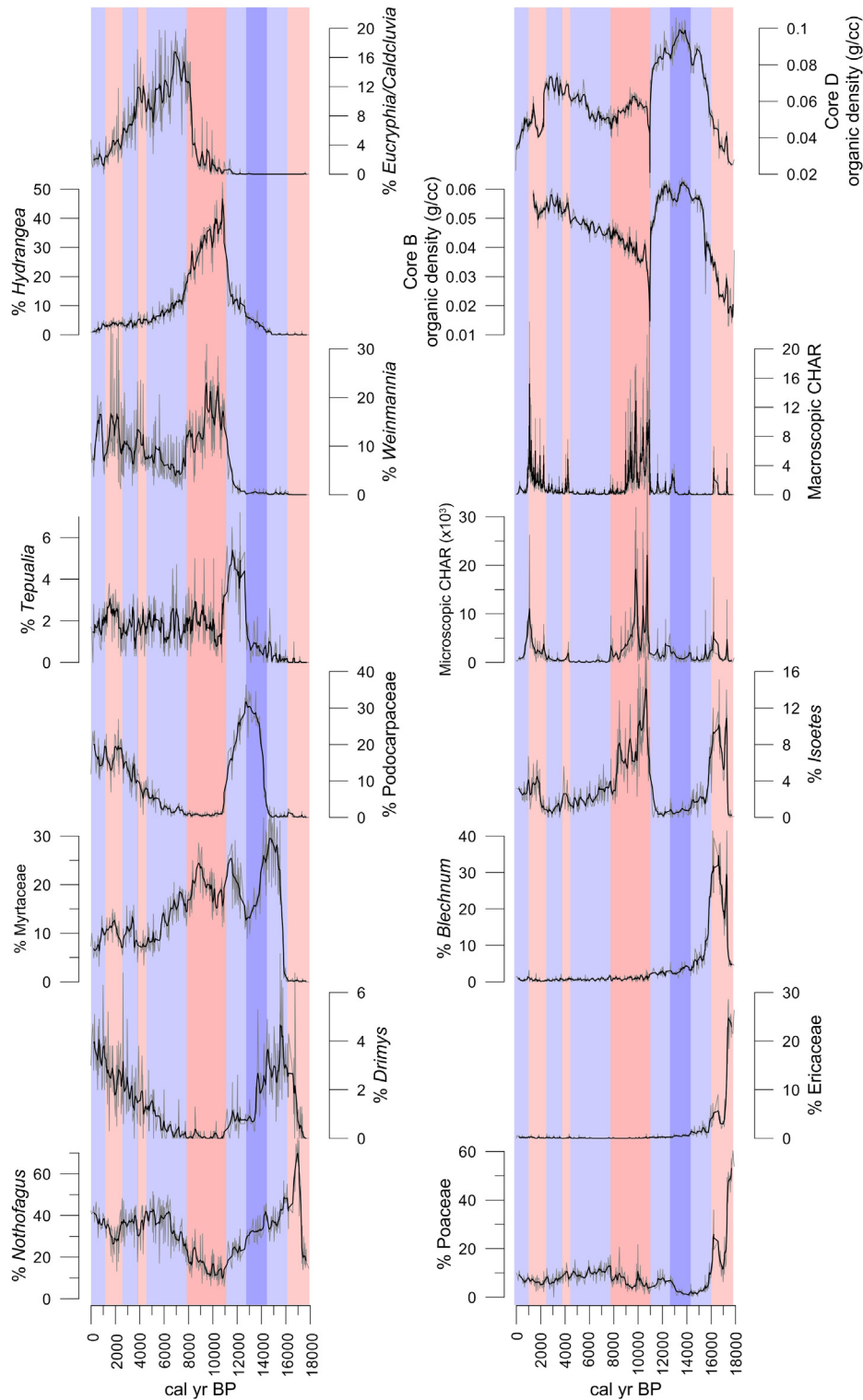


Fig. 8. Selected variables from the Lago Lepu  record expressed in a common timescale. Red rectangles represent relatively dry intervals; blue rectangles represent relatively wet intervals. The raw values for each time series is shown in gray, the black solid lines represent weighted 7-point weighted running means applied to each record. (For interpretation of the references to colour in this figure legend, the reader is referred to the web version of this article.)

drop. Collectively, our data suggest that the interval 7800–11,000 cal yr BP was the warmest/driest multi-millennial period of the entire Lago Lepu  record.

Ignition sources in these broad-leaved temperate rainforest ecosystems are related to the incendiary effects of volcanic ash

deposition, lightning strikes and human activities. Volcanic disturbance can be out ruled as the main driver of paleofires in Isla Grande de Chilo  owing the >100 km distance to the nearest eruptive center and the fact that three tephras cannot account for the centennial and millennial-scale changes in CHAR over the last

17,800 years. Lightning associated with modes of variability such as the Southern Annular Mode can provide the necessary conditions for ignition even under the cool-temperate and wet environments of Isla Grande de Chiloé (Holz and Veblen, 2012). Human burning over the Holocene is likely taking into account the abundance of coastal archeological sites in the region. Attribution of Pleistocene fires to human activities is less certain considering that only one site in the entire region, located 150 km northeast of Lago Lepué, contains remains of putative human origin dated at ~14,000 cal yr BP (Dillehay, 1997).

4.2. Regional implications

Comparison between four diagnostic taxa (*Eucryphia/Caldcluvia*, *W. trichosperma*, *Nothofagus*, and podocarps) from the Lago Lepué and L. Condorito pollen records (Moreno, 2004) reveals coherence of vegetation and climate change at millennial and multi-millennial

scales over the last ~14,000 years (Fig. 9). We note, however, that variations in *Eucryphia/Caldcluvia* and *W. trichosperma* occurred earlier, faster and were larger in magnitude in the L. Condorito record. Because stratigraphic and chronologic control is precise in both sites, both are small closed-basin lakes located on top of low-elevation LGM moraines, and migrational lags can be ruled out as both species were present in low abundance prior to their respective increases in each site, we propose that a gradient in temperature and summer moisture stress prevalent along this ~135 km-long transect acted as a filter for shade-intolerant Valdivian rainforest trees capable of colonizing forest gaps generated by fire disturbance. Other Chilotan sites located within ~20 km (L. Tahui and L. Melli) (Abarzua et al., 2004; Abarzua and Moreno, 2008) show a behavior similar to L. Lepué suggesting this signal is representative at the landscape level in central-east Isla Grande de Chiloé. We conclude that the warm/dry multi-millennial phase between 7800 and 11,000 cal yr BP was more pronounced near L.

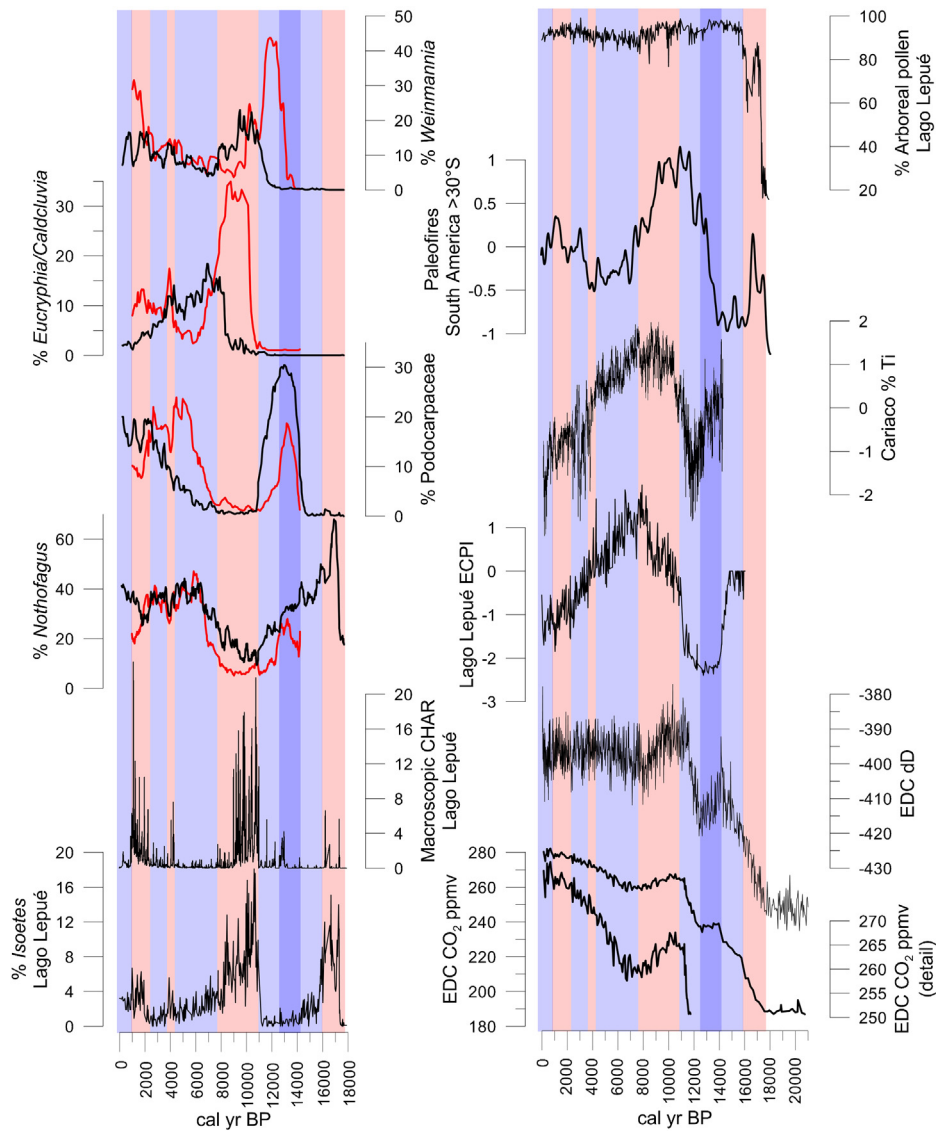


Fig. 9. Left panel: comparison of selected variables from Lago Lepué (black lines) with the Lago Condorito record (red lines). The % *Weinmannia trichosperma*, % *Eucryphia/Caldcluvia*, % *Podocarpaceae* and % *Nothofagus* curves are weighted 7-point weighted running means applied to each record. Right panel: comparison of the ECPI and arboreal pollen curve from Lago Lepué with the standardized paleofire curve from southern South America, the %Titanium from Cariaco Basin, and the δ Deuterium and atmospheric CO₂ records from the Antarctic EPICA Dome Concordia ice core. Red rectangles represent relatively dry intervals; blue rectangles represent relatively wet intervals. (For interpretation of the references to colour in this figure legend, the reader is referred to the web version of this article.)

Condorito, located further north than L. Lepu , favoring the Valdivian taxon *Eucryphia/Caldcluvia* whereas the pioneer shade-intolerant species *W. trichosperma* was able to occupy forest gaps in the relatively cooler and moister sectors of central-east Isla Grande de Chilo .

In the following paragraphs we address the questions we lay out in the introduction about the paleoenvironmental evolution of northwestern Patagonia.

- 1 When did ice-free conditions begin in central-east Isla Grande de Chilo  during the Last Glacial termination? Identical AMS dates from two separate cores from the deepest sector of Lago Lepu  afford minimum limiting ages of ~17,800 cal yr BP for the onset of organic sedimentation in a sector formerly covered by the Golfo de Corcovado piedmont glacier lobe during the LGM. These results constrain the timing for the onset of local ice-free conditions during the Last Glacial termination, and are congruent with similar results from the Mayol Bog (Heusser et al., 1999), located 20 km north from Lago Lepu  (Fig. 1), and the recessional chronology from the Lago Llanquihue, Seno Reloncav  and Golfo de Ancud piedmont glacier lobes during the last termination (Denton et al., 1999). These results suggest that the warm event at ~17,800 cal yr BP was a decisive trigger for widespread deglaciation from the lowlands of northwestern Patagonia during the last termination.
- 2 How fast did forest vegetation establish during the Last Glacial termination? Our results indicate a basal assemblage dominated by cold-resistant shrubs and herbs between 17,400 and 17,800 cal yr BP, established immediately after this sector of Isla Grande de Chilo  became ice free, along with persistently low *Nothofagus* (~25%). This was followed by an exponential increase in *Nothofagus* that led to ~90% dominance of arboreal pollen by 17,000 cal yr BP. Palynological results from the Canal de la Puntilla and Huelmo sites show a deglacial *Nothofagus* rise immediately after recession from the LGM margins at ~17,800 cal yr BP (Moreno et al., 1999; Moreno and Leon, 2003), unlike Lago Lepu  these sites were located in the periphery of the ice margins during the LGM. It appears then that the ~400-year long difference for the onset of the *Nothofagus* rise in central-east Isla Grande de Chilo  might represent a migrational lag from the source populations located in sectors distal to the western margin of the Golfo de Corcovado piedmont glacier lobe.
- 3 Was the deglacial warming trend a monotonic/unidirectional process? The abruptness and irreversibility of arboreal expansion and subsequent persistence of rainforest vegetation strongly suggest rapid warming at the onset of the Last Glacial termination. Closed-canopy forests dominated between 14,600 and 17,000 cal yr BP under temperate and wet conditions followed by a reversal toward cooler and wetter conditions between 11,500 and 14,600 cal yr BP, the first part of which featured the largest magnitude decline in temperature between 12,700 and 14,600 cal yr BP. Warming at 11,500 cal yr BP initiated interglacial climate in the region. Thus, deglacial warming was punctuated by cold pulses and variations in the amount of precipitation delivered by the SWW at millennial timescales (Moreno et al., 2001) which did not alter the predominance but changed the species composition of temperate rainforests in central-east Isla Grande de Chilo .
- 4 How did the SWW vary through the transition from extreme glacial to extreme interglacial conditions? Because local precipitation exhibits a strong positive correlation with zonal SWW speeds in this part of Patagonia, we can use this modern relationship to infer past SWW strength/position based on paleoprecipitation estimates. The Lago Lepu  record shows high

abundance of the littoral macrophyte *Isoetes* between 16,100 and 17,400 cal yr BP suggesting low lake levels, superseded by increases in the hygrophilous conifer *Fitzroya/Pilgerodendron*, other hygrophilous trees and decline in *Isoetes* indicating abundant precipitation and higher lake levels. A further increase in precipitation is inferred from the rise of the hygrophilous cold-resistant *P. nubigena* between 12,700 and 14,600 cal yr BP, followed by a decline in precipitation associated with paleofires, increases in trees commonly found in waterlogged environments associated with lake margins (Myrtaceae, *T. stipularis*) and a decline in *P. nubigena* between 11,500 and 12,700 cal yr BP. Disappearance of *P. nubigena*, increases in tree species with broad climatic tolerance, intense fire activity and a prominent increase in the littoral macrophyte *Isoetes* during the interval 7800–11,000 cal yr BP defines the warmest/driest multi-millennial period in the Lago Lepu  record. In sum, our data indicate millennial-scale changes in precipitation and SWW influence through the Last Glacial termination with low levels immediately after its onset, followed by increments at 16,100 and 14,600 cal yr BP and declines at 12,700 and 11,500 cal yr BP. Minimum precipitation and SWW influence is evident between 7800 and 11,000 cal yr BP, consistent with earlier studies (Moreno and Leon, 2003; Moreno, 2004).

- 5 Is there evidence for high-frequency changes in the SWW during the Holocene? Changes in terrestrial and aquatic vegetation suggest hydroclimate variations at millennial timescales during the Holocene, with prominent shifts at 800, 1700, 2500, 4000–4300, 6200, 7800, 8600 and 10,000 cal yr BP. Centennial-scale changes are evident in the organic density data from the intermediate and deep sectors of the lake, following a conspicuous multi-millennial shift at 6200 cal yr BP. Although the origin of these oscillations is currently unknown, we suspect they involve productivity changes in the lake induced by varying hydroclimate conditions, which in this sector of Patagonia are ultimately linked to fluctuations in the strength and seasonality of the SWW.
- 6 How did fire regimes shift through these transitions or climatic states? We observe intermittent centennial-scale shifts in fire regime at millennial timescales during predominantly cold-temperate and wet multi-millennial intervals, associated with reversible vegetation changes. Sustained, large-magnitude increases prevail during warm/dry multi-millennial intervals and are associated with major shifts in the composition and structure of the vegetation, suggesting positive feedbacks between enhanced fire activity and vegetation change.

4.3. Hemispheric and global implications

In this section we examine the timing and direction of hydroclimate variations inferred from Lago Lepu  and their implications in the context of low and high latitude variations in the Southern Hemisphere. Our primary criteria are changes in littoral macrophytes and upland vegetation, fire-regime shifts and sediment limit variations discussed in the preceding sections. The *Eucryphia/Caldcluvia* versus Podocarpaceae (*P. nubigena* + *S. conspicua*) index (ECPI), standardized to the mean of the entire record, quantifies the degree of mixture between North Patagonian and Valdivian rainforests and serves as a diagnostic of hydroclimate variations in central-east Isla Grande de Chilo  over the last ~16,100 years (Moreno, 2004) (Fig. 9). Applicability of the ECPI is restricted to the interval when North Patagonian and/or Valdivian rainforests had already established near Lago Lepu , hence the following analysis excludes the interval 16,100–17,800 cal yr BP. At multi-millennial timescales the ECPI shows slightly negative or zero anomalies

between 14,600 and 16,100 cal yr BP, followed by a rapid decline that led to strongly negative anomalies at 12,700 cal yr BP. These results indicate that cold-wet conditions during the Last Glacial termination intensified between 12,700 and 14,600 cal yr BP and attenuated slightly between 11,000 and 12,700 cal yr BP. An abrupt increase in ECPI started at ~11,000 cal yr BP and was followed by a gradual and sustained increase to peak positive anomalies at ~7800 cal yr BP, after which the ECPI descends steadily toward the present. Increasingly positive anomalies in ECPI between ~7800 and 11,000 cal yr BP suggest a decline in precipitation and increase in temperature, followed by a sustained decline indicative of colder, wetter conditions.

We interpret negative anomalies in precipitation during the earliest portion of the Last Glacial termination (16,100–17,800 cal yr BP) in Lago Lepu e as a southward shift of the SWW from an equatorward-displaced position during the LGM. Such shift was contemporaneous with the onset of deglacial warming and CO₂ rise (Monnin et al., 2001) (Fig. 9) and increase in diatom productivity in the Southern Ocean (Anderson et al., 2009), lending support to the hypothesis that wind stress imparted by the SWW on the surface of the Southern Ocean was a decisive trigger for upwelling and ventilation of CO₂-enriched deep waters (Toggweiler et al., 2006; Toggweiler, 2009). An increase in precipitation ensued at 16,100 cal yr BP following the establishment of closed-canopy *Nothofagus* forest by 17,000 cal yr BP reflecting a northward shift or strengthening of the SWW.

Slightly negative ECPI values between 14,600 and 16,100 cal yr BP indicate predominance of North Patagonian rainforest vegetation with a minor component of cold-resistant hygrophilous podocarps and virtual absence of the littoral macrophyte *Isoetes*; this was followed by strongly negative ECPI values between 12,700 and 14,600 cal yr BP which we interpret as an equatorward shift of the SWW implying cooler climate and further increase in SWW influence in Lago Lepu e during ACR time. We note this shift was synchronous with similar changes in paleoecological records from the  ltima Esperanza sector of southwestern Patagonia (Moreno et al., 2012) and glacial readvances in the same region (Moreno et al., 2009; Strelin et al., 2011) and the Southern Alps of New Zealand (Putnam et al., 2010). We hypothesize that a northward shift in the SWW might have diminished upwelling of CO₂-rich deep waters and ventilation in the Southern Ocean causing a pause in the deglacial atmospheric CO₂ rise shown in Antarctic ice cores while the % Ti from Cariaco Basin, interpreted as a measure of the mean latitude of the Intertropical Convergence Zone (ITCZ) in tropical South America (Haug et al., 2001), shows average values relative to the mean of the entire record (Fig. 9). A moderate rise in ECPI is evident in the Lago Lepu e record between ~11,500 and 12,700 cal yr BP, suggesting slightly less SWW influence which was coeval with a rise in fire activity in southern South America (Power et al., 2008), a southward shift in the ITCZ implied by strongly negative anomalies in % Ti from Cariaco, increased SWW influence in southwestern Patagonia, glacial recession in the same region and in the Southern Alps of New Zealand (Moreno et al., 2009; Kaplan et al., 2010; Strelin et al., 2011; Moreno et al., 2012), renewed Antarctic warming and resumption of the atmospheric CO₂ rise (Monnin et al., 2004), suggesting a poleward shift of the SWW that might have increased upwelling and outgassing of CO₂ in the Southern Ocean.

Abrupt increases in *Isoetes*, charcoal and ECPI at ~11,500 cal yr BP led to prominent maxima during the early Holocene, defining the warmest/driest interval in the entire Lago Lepu e record that coincides with a zonally symmetric multi-millennial phase featuring weak SWW circulation between 7800 and 11,000 cal yr BP (Fletcher and Moreno, 2011). This was

contemporaneous with peak Antarctic air temperatures and precipitation in tropical South America associated with a northward shift of the ITCZ. The Lago Lepu e record then shows sustained declines in *Isoetes*, charcoal and ECPI starting at ~7800 cal yr BP (Fig. 9), suggesting a multi-millennial decline in temperature and increase in precipitation associated with a zonally symmetric strengthening of the SWW (Fletcher and Moreno, 2011) overprinted by millennial and centennial-scale oscillations. Antarctic temperatures have remained relatively invariant since ~7800 cal yr BP contemporaneous with a gradual rise in atmospheric CO₂; the Cariaco Basin record, on the other hand, shows a sustained southward shift of the ITCZ (Fig. 9).

We propose that tropical and high-latitude controls have affected the position and strength of the SWW over the last ~18,000 years. Millennial-scale changes in the SWW correspond with important events in Antarctica through the last termination, i.e. poleward shift during the onset of deglacial warming and during YD time, northward shift during ACR time. A close coupling is also evident with multi-millennial changes in the latitudinal position of the ITCZ in the South American sector over the last ~12,700 years. We observe that the SWW became stronger or shifted northward when the ITCZ migrated south, and viceversa, suggesting that latitudinal shifts of the climatic equator affected baroclinicity in the Southern Hemisphere, invigorating or weakening the SWW over the last ~12,700 years.

5. Conclusions

- Recession of the Golfo Corcovado ice lobe during the Last Glacial termination exposed the central-east sector of Isla Grande de Chilo e at 17,800 cal yr BP.
- Ice-free conditions allowed the immediate colonization of pioneer herbs and shrubs, followed by rapid establishment of closed-canopy *Nothofagus* forests between 17,000 and 17,400 cal yr BP.
- Evergreen forests have dominated the region since 17,000 cal yr BP with variations in their structure and composition that suggest alternation and subsequent mixing of North Patagonian and Valdivian rainforest communities. These changes were driven primarily by changes in temperature and the amount/seasonality of precipitation.
- Low lake levels and enhanced fire activity between 800 and 2000, 4000–4300, ~8000–11,000 and 16,100–17,800 cal yr BP suggest lowered precipitation in northwestern Patagonia. The interval between 8000 and 11,000 cal yr BP constitutes the warmest/driest phase in central-east Isla Grande de Chilo e and northwestern Patagonia. Precipitation increased in the intervening millennia, implying northward shifts or intensification of the SWW.
- Considering the positive correlation between zonal wind speeds and local precipitation, we infer that the SWW influence was reduced between 800–2000, 4000–4300, ~8000–11,000 and 16,100–17,800 cal yr BP at this latitude (43 S), and increased in the intervening millennia.
- We detect cooling and increased precipitation during the ACR, suggesting a northward shift of the SWW, and attenuation of these changes during Younger Dryas time, suggesting a southward shift of the SWW along with enhanced rainfall seasonality and fire activity.
- Millennial and centennial-scale changes during the Holocene suggest highly variable hydroclimate conditions in central-east Isla Grande de Chilo e, most likely reflecting meridional changes in the SWW.
- Covariation in paleoclimate trends revealed by the Lago Lepu e record with tropical and Antarctic records over the last 18,000

years, suggests that the SWW are a highly dynamic component of the climate system capable of linking paleoclimate changes from low- and high-latitudes during the Last Glacial termination and the current interglacial.

Acknowledgements

This research was funded by Fondecyt grant #1110612, Fondap grant #15110009, and ICM grants PO2-51 and NC120066. We thank R. Villa, R. Flores, A. León, A. Maldonado and M. Valenzuela for help during the coring operation, and L. Gonzalorenza, and L. Hernández for laboratory analyses. I. Hajdas, C. Moy and T. Guilderson contributed in the development of the radiocarbon chronology.

References

- Abarzua, A.M., Moreno, P.I., 2008. Changing fire regimes in the temperate rainforest region of southern Chile over the last 16,000 yr. *Quat. Res.* 69, 62–71.
- Abarzua, A.M., Villagran, C., Moreno, P.I., 2004. Deglacial and postglacial climate history in east-central Isla Grande de Chiloe, southern Chile (43 degrees S). *Quat. Res.* 62, 49–59.
- Aguas, D.G.d., 1987. Balance hídrico de Chile: 1987. Ministerio de Obras Públicas, Chile.
- Anderson, R.F., Ali, S., Bradtmiller, L.L., Nielsen, S.H.H., Fleisher, M.Q., Anderson, B.E., Burckle, L.H., 2009. Wind-driven upwelling in the southern ocean and the deglacial rise in atmospheric CO₂. *Science* 323, 1443–1448.
- Bennett, K.D., Haberle, S.G., Lumley, S.H., 2000. The last glacial-Holocene transition in Southern Chile. *Science* 290, 325–328.
- Blaauw, M., Christen, J.A., 2011. Flexible paleoclimate age-depth models using an autoregressive gamma process. *Bayesian Anal.* 6, 457–474.
- Denton, G.H., Anderson, R.F., Toggweiler, J.R., Edwards, R.L., Schaefer, J.M., Putnam, A.E., 2010. The last glacial termination. *Science* 328, 1652–1656.
- Denton, G.H., Lowell, T.V., Heusser, C.J., Schluchter, C., Andersen, B.G., Heusser, L.E., Moreno, P.I., Marchant, D.R., 1999. Geomorphology, stratigraphy, and radiocarbon chronology of Llanquihue drift in the area of the southern Lake District, Seno Reloncavi, and Isla Grande de Chiloe, Chile. *Geogr. Ann. Ser. A-Phys. Geogr.* 81A, 167–229.
- Dillehay, T., 1997. Monte Verde. A Late Pleistocene Settlement in Chile. The Archaeological Context and Interpretation. Smithsonian Institution Press, Washington.
- Faegri, K., Iversen, J., 1989. *Textbook of Pollen Analysis*. John Wiley & Sons.
- Fletcher, M.S., Moreno, P.I., 2011. Zonally symmetric changes in the strength and position of the Southern Westerlies drove atmospheric CO₂ variations over the past 14 k.y. *Geology* 39, 419–422.
- García, J.L., Kaplan, M.R., Hall, B.L., Schaefer, J.M., Vega, R.M., Schwartz, R., Finkel, R., 2012. Glacier expansion in southern Patagonia throughout the Antarctic cold reversal. *Geology* 40, 859–862.
- Garreaud, R.D., 2007. Precipitation and circulation covariability in the extratropics. *J. Clim.* 20, 4789–4797.
- Godley, E.J., Moar, N.T., 1973. Vegetation and pollen analysis of two bogs on Chiloe. *N. Z. J. Bot.* 11, 255–268.
- Hajdas, I., Bonani, G., Moreno, P.I., Ariztegui, D., 2003. Precise radiocarbon dating of late-glacial cooling in mid-latitude South America. *Quat. Res.* 59, 70–78.
- Haug, G.H., Hughen, K.A., Sigman, D.M., Peterson, L.C., Röhl, U., 2001. Southward migration of the intertropical convergence zone through the holocene. *Science* 293, 1304–1308.
- Heusser, C.J., 1990. Chilotan piedmont glacier in the Southern Andes during the Last Glacial Maximum. *Rev. Geol. Chile* 17, 3–18.
- Heusser, C.J., 1994. Paleoindians and fire during the late Quaternary in southern south-America. *Rev. Chil. Hist. Nat.* 67, 435–443.
- Heusser, C.J., Denton, G.H., Hauser, A., Andersen, B.G., Lowell, T.V., 1995. Quaternary pollen records from the Archipiélago de Chiloe in the context of glaciation and climate. *Rev. Geol. Chile* 22, 25–46.
- Heusser, C.J., Flint, R.F., 1977. Quaternary glaciations and environments of northern Isla Chiloe. *Geology* 5, 305–308.
- Heusser, C.J., Heusser, L.E., Lowell, T.V., 1999. Paleoecology of the southern Chilean Lake District-Isla Grande de Chiloe during middle-Late Llanquihue glaciation and deglaciation. *Geogr. Ann. Ser. A-Phys. Geogr.* 81 A, 231–284.
- Heusser, C.J., Streeter, S.S., Stuiver, M., 1981. Temperature and precipitation record in southern Chile extended to 43,000 ago. *Nature* 294, 65–67.
- Holz, A., Veblen, T.T., 2012. Wildfire activity in rainforests in western Patagonia linked to the Southern Annular Mode. *Int. J. Wildland Fire* 21, 114–126.
- Holling, J.T., Schilling, D.H., 1981. Late Wisconsin-Weichselian mountain glaciers and small ice caps. In: Denton, G.H., Hughes, T.J. (Eds.), *The Last Great Ice Sheets*. Wiley Interscience, pp. 179–206.
- Kaplan, M.R., Schaefer, J.M., Denton, G.H., Barrell, D.J.A., Chinn, T.J.H., Putnam, A.E., Andersen, B.G., Finkel, R.C., Schwartz, R., Doughty, A.M., 2010. Glacier retreat in New Zealand during the Younger Dryas stadial. *Nature* 467, 194–197.
- Lamy, F., Kaiser, J., Ninnemann, U., Hebbeln, D., Arz, H.W., Stoner, J., 2004. Antarctic timing of surface water changes off Chile and Patagonian Ice Sheet response. *Science* 304, 1959–1962.
- Markgraf, V., Huber, U.M., 2011. Late and postglacial vegetation and fire history in Southern Patagonia and Tierra del Fuego. *Palaeogeogr. Palaeoclimatol. Palaeoecol.* 297, 351–366.
- Markgraf, V., Iglesias, V., Whitlock, C., 2013. Late and postglacial vegetation and fire history from Cordón Serrucho Norte, northern Patagonia. *Palaeogeogr. Palaeoclimatol. Palaeoecol.* 371, 109–118.
- Mercer, J.H., 1965. Glacier variations in southern Patagonia. *Geogr. Rev.* 55, 390–413.
- Monnin, E., Indermuhle, A., Dallenbach, A., Fluckiger, J., Stauffer, B., Stocker, T.F., Raynaud, D., Barnola, J.M., 2001. Atmospheric CO₂ concentrations over the last glacial termination. *Science* 291, 112–114.
- Monnin, E., Steig, E.J., Siegenthaler, U., Kawamura, K., Schwander, J., Stauffer, B., Stocker, T.F., Morse, D.L., Barnola, J.M., Bellier, B., Raynaud, D., Fischer, H., 2004. Evidence for substantial accumulation rate variability in Antarctica during the Holocene, through synchronization of CO₂ in the Taylor Dome, Dome C and DML ice cores. *Earth Planet. Sci. Lett.* 224, 45–54.
- Montecinos, A., Aceituno, P., 2003. Seasonality of the ENSO-related rainfall variability in Central Chile and associated circulation anomalies. *J. Clim.* 16.
- Moreno, P.I., 2004. Millennial-scale climate variability in northwest Patagonia over the last 15000 yr. *J. Quat. Sci.* 19, 35–47.
- Moreno, P.I., Jacobson, G.L., Lowell, T.V., Denton, G.H., 2001. Interhemispheric climate links revealed by a late-glacial cooling episode in southern Chile. *Nature* 409, 804–808.
- Moreno, P.I., Kaplan, M.R., Francois, J.P., Villa-Martinez, R., Moy, C.M., Stern, C.R., Kubik, P.W., 2009. Renewed glacial activity during the Antarctic cold reversal and persistence of cold conditions until 11.5 ka in southwestern Patagonia. *Geology* 37, 375–378.
- Moreno, P.I., Leon, A.L., 2003. Abrupt vegetation changes during the last glacial to Holocene transition in mid-latitude South America. *J. Quat. Sci.* 18, 787–800.
- Moreno, P.I., Lowell, T.V., Jacobson, G.L., Denton, G.H., 1999. Abrupt vegetation and climate changes during the last glacial maximum and last termination in the Chilean Lake District: a case study from Canal de la Puntilla (41 degrees S). *Geogr. Ann. Ser. A-Phys. Geogr.* 81A, 285–311.
- Moreno, P.I., Villa-Martinez, R., Cardenas, M.L., Sagredo, E.A., 2012. Deglacial changes of the southern margin of the southern westerly winds revealed by terrestrial records from SW Patagonia (52 degrees S). *Quat. Sci. Rev.* 41, 1–21.
- Moy, C.M., Dunbar, R.B., Moreno, P.I., Francois, J.P., Villa-Martinez, R., Mucciarone, D.M., Guilderson, T.P., Garreaud, R.D., 2008. Isotopic evidence for hydrologic change related to the westerlies in SW Patagonia, Chile, during the last millennium. *Quat. Sci. Rev.* 27, 1335–1349.
- Power, M.J., Marlon, J., Ortiz, N., Bartlein, P.J., Harrison, S.P., Mayle, F.E., Ballouche, A., Bradshaw, R.H.W., Carcaillet, C., Cordova, C., Mooney, S., Moreno, P.I., Prentice, I.C., Thonicke, K., Tinner, W., Whitlock, C., Zhang, Y., Zhao, Y., Ali, A.A., Anderson, R.S., Beer, R., Behling, H., Briles, C., Brown, K.J., Brunelle, A., Bush, M., Camill, P., Chu, G.Q., Clark, J., Colombaroli, D., Connor, S., Daniaou, A.L., Daniels, M., Dodson, J., Doughty, E., Edwards, M.E., Finsinger, W., Foster, D., Frechette, J., Gaillard, M.J., Gavin, D.G., Gobet, E., Haberle, S., Hallett, D.J., Higuera, P., Hope, G., Horn, S., Inoue, J., Kaltenrieder, P., Kennedy, L., Kong, Z.C., Larsen, C., Long, C.J., Lynch, J., Lynch, E.A., McGlone, M., Meeks, S., Mensing, S., Meyer, G., Minckley, T., Mohr, J., Nelson, D.M., New, J., Newnham, R., Noti, R., Oswald, W., Pierce, J., Richard, P.J.H., Rowe, C., Goni, M.F.S., Shuman, B.N., Takahara, H., Toney, J., Turney, C., Urrego-Sanchez, D.H., Umbanhowar, C., Vandergoes, M., Vanniene, B., Vescovi, E., Walsh, M., Wang, X., Williams, N., Wilmshurst, J., Zhang, J.H., 2008. Changes in fire regimes since the Last Glacial Maximum: an assessment based on a global synthesis and analysis of charcoal data. *Clim. Dyn.* 30, 887–907.
- Putnam, A.E., Denton, G.H., Schaefer, J.M., Barrell, D.J.A., Andersen, B.G., Finkel, R.C., Schwartz, R., Doughty, A.M., Kaplan, M.R., Schluchter, C., 2010. Glacier advance in southern middle-latitudes during the Antarctic Cold Reversal. *Nat. Geosci.* 3, 700–704.
- Quintana, J.M., Aceituno, P., 2012. Changes in the rainfall regime along the extra-tropical west coast of South America (Chile): 30–43 degrees S. *Atmosfera* 25, 1–22.
- Sagredo, E.A., Moreno, P.I., Villa-Martinez, R., Kaplan, M.R., Kubik, P.W., Stern, C.R., 2011. Fluctuations of the Ultima Esperanza ice lobe (52 degrees S), Chilean Patagonia, during the last glacial maximum and termination 1. *Geomorphology* 125, 92–108.
- Shuman, B., 2003. Controls on loss-on-ignition variation in cores from two shallow lakes in the northeastern United States. *J. Paleolimnol.* 30, 371–385.
- Stenni, B., Masson-Delmotte, V., Selmo, E., Oerter, H., Meyer, H., Rothlisberger, R., Jouzel, J., Cattani, O., Falourd, S., Fischer, H., Hoffmann, G., Iacumin, P., Johnsen, S.J., Minster, B., Udisti, R., 2010. The deuterium excess records of EPICA Dome C and Dronning Maud Land ice cores (East Antarctica). *Quat. Sci. Rev.* 29, 146–159.
- Stern, C.R., Moreno, P.I., Villa-Martinez, R., Sagredo, E.A., Prieto, A., Labarca, R., 2011. Evolution of ice-dammed proglacial lakes in Ultima Esperanza, Chile: implications from the late-glacial R1 eruption of Reclus volcano, Andean Austral Volcanic Zone. *Andean Geol.* 38, 82–97.
- Strelin, J.A., Denton, G.H., Vandergoes, M.J., Ninnemann, U.S., Putnam, A.E., 2011. Radiocarbon chronology of the late-glacial puerto Bandera moraines, southern Patagonian Icefield, Argentina. *Quat. Sci. Rev.* 30, 2551–2569.
- Toggweiler, J.R., 2005. Climate change from below. *Quat. Sci. Rev.* 24, 511–512.
- Toggweiler, J.R., 2009. Shifting westerlies. *Science* 323, 1434–1435.

- Toggweiler, J.R., Russell, J.L., Carson, S.R., 2006. Midlatitude westerlies, atmospheric CO₂, and climate change during the ice ages. *Paleoceanography* 21. <http://dx.doi.org/10.1029/2005PA001154>.
- Villagrán, C., 1985. Análisis palinológico de los cambios vegetacionales durante el Tardiglacial y Postglacial en Chiloé, Chile. *Rev. Chil. Hist. Nat.* 58, 57–69.
- Villagrán, C., 1988a. Expansion of Magellanic moorland during the Late Pleistocene: palynological evidence from northern Isla Grande de Chiloé, Chile. *Quat. Res.* 30, 304–314.
- Villagrán, C., 1988b. Late Quaternary vegetation of Southern Isla Grande de Chiloé, Chile. *Quat. Res.* 29, 294–306.
- Villagrán, C., 2001. Un modelo de la historia de la vegetación de la Cordillera de la Costa de Chile central-sur: la hipótesis glacial de Darwin. *Rev. Chil. Hist. Nat.* 74, 793–803.
- Whitlock, C., Bianchi, M.M., Bartlein, P.J., Markgraf, V., Marlon, J., Walsh, M., McCoy, N., 2006. Postglacial vegetation, climate, and fire history along the east side of the Andes (lat 41–42.5°S), Argentina. *Quat. Res.* 66, 187–201.
- Whitlock, C., Moreno, P.I., Bartlein, P., 2007. Climatic controls of Holocene fire patterns in southern South America. *Quat. Res.* 68, 28–36.